



# Thermodynamic Parameters of Non-isothermal Degradation of a New Family of Organometallic Dendrimer with Isoconversional Methods

Ahmad A. Joraid<sup>1</sup> · Rawda M. Okasha<sup>2</sup> · Mahdi A. Al-Maghrabi<sup>3</sup> · Tarek H. Affi<sup>2</sup> · Christian Agatemor<sup>4</sup> · Alaa S. Abd-El-Aziz<sup>5</sup>

Received: 28 December 2021 / Accepted: 18 March 2022 / Published online: 11 April 2022  
© The Author(s), under exclusive licence to Springer Science+Business Media, LLC, part of Springer Nature 2022

## Abstract

The objective of this work is to obtain the thermodynamic parameters (the changes in enthalpy, Gibbs free energy, and entropy) of two degradation steps observed in three novel families of organometallic dendrimers. The isoconversional Flynn–Wall–Ozawa (FWO) model was employed to calculate the effective activation energy and pre-exponential factor. The changes in enthalpy and the entropy revealed a quite consistent tendency with the activation energy whereas the change of Gibbs free energy always remained positive during the whole degradation process, which demonstrated the implication that the degradation is non-spontaneous and thus requires an external heat supply.

**Keywords** Dendrimers · Thermogravimetric analysis · Isoconversional methods · Nonisothermal kinetics · Thermodynamic parameters

## 1 Introduction

Dendrimers are large monodisperse highly-branched molecules with precisely designed and defined homogeneous structures. Due to its unique chemical properties, dendrimers have been established as a critical material and have been actively researched during recent years. With their globular topology and tailored peripheral end groups, dendrimers have been employed in several applications, including: pharmaceutical drug and gene delivery, chemotherapy, and diagnostic imaging [1–5]. While a majority of the synthesized dendrimers are organic macromolecules, great efforts

have unveiled the incorporation of inorganic elements, transition metals, and organometallic entities in order to generate inorganic and organometallic dendrimers. Case in point, this research merges the properties of these inorganic central elements and organometallic entities/fragments, such as catalytic; electrochemical; optical; and magnetic properties, with the benefits generally attributed to dendrimers, such as site isolation; precise steric environments; recyclability; and possible cooperative effects [6].

The study of the thermodynamic characteristics of dendrimers in a wide range of temperatures has allowed the detection and analysis of certain changes of practical significance in the properties of compounds, depending on their compositions and structures [7–10]. This study is a continuation to our preceding study on organometallic dendrimers, exemplified by a new family of cross-linked organoiron dendrimers [5]. Understanding dendrimer degradation is extremely important as degradation dictates dendrimer stability during synthesis, processing, fabrication, and applications. Although there is sufficient research regarding dendrimer stability and processing, current research into dendrimer degradation lacks the synthesis and application facilities, creating a gap that limits real-life applications. In contrast, polymer degradation has been extensively researched, which includes a magnifying glass surrounding their kinetics and thermodynamics of this process. Our

✉ Ahmad A. Joraid  
aaljoraid@taibahu.edu.sa

<sup>1</sup> Physics Department, Faculty of Science, Taibah University, Al-Madinah Al-Munawarah 30002, Saudi Arabia

<sup>2</sup> Chemistry Department, Faculty of Science, Taibah University, Al-Madinah Al-Munawarah 30002, Saudi Arabia

<sup>3</sup> Department of General Studies, Yanbu Industrial College, Yanbu, Saudi Arabia

<sup>4</sup> Chemistry Department, University of Miami, Coral Gables, FL, USA

<sup>5</sup> Chemistry Department, Faculty of Science, University of Prince Edward Island, Charlottetown, Prince Edward Island C1A 4P3, Canada

earlier work resulted in the synthesis of a class of organometallic dendrimers (a special class of polymers) and encompassed the characterization of the kinetics of the degradation process, which specifies the determination of their kinetic triplets, pre-exponential (frequency) factors, effective activation energies, and reaction models. However, the previous report did not explore the optimization of the degradation processes via the quantification of the thermodynamic parameters.

Thus, the primary objective of this article is to quantify the thermodynamic parameters, which encompass the changes in enthalpy ( $\Delta H$ ), Gibbs free energy ( $\Delta G$ ), and entropy ( $\Delta S$ ). These parameters were calculated through the nonisothermal degradation of a novel moiety of organometallic dendrimers. The values of the effective activation energy and the pre-exponential factor were similarly acquired, utilizing the isoconversional Flynn–Wall–Ozawa (FWO) methodology.

## 2 Materials and Methods

### 2.1 Materials

All chemicals and reagents were attained from Sigma-Aldrich. Pentaerythritol, 4,4'-bis(4-hydroxyphenyl)valeric acid, magnesium sulfate, ammonium hexafluorophosphate ( $\text{NH}_4\text{PF}_6$ ), potassium carbonate, 4-(dimethylamino)pyridine (DMAP), *N,N'*-dicyclohexylcarbodiimide (DCC), diethyl ether, acetone, chloroform, and hydrogen chloride acid were used as received. Dimethyl sulfoxide- $d_6$  ( $\text{DMSO-}d_6$ ) was distilled over calcium hydride. Dimethyl sulfoxide (DMSO), Dichloromethane (DCM) was purified by passing the solvent through an Innovative Technology solvent purification system that consists of columns of alumina and copper catalyst. *N,N'*-dimethylformamide (DMF) were dried, and stored over 3 Å molecular sieve before being used.

### 2.2 Instrumentation

$^1\text{H}$ - and  $^{13}\text{C}$ -NMR spectra were recorded at 400 and 125 MHz, respectively, on a Gemini 200 NMR spectrometer, with chemical shifts calculated in Hz, referenced to solvent residues. The IR spectra of the new compounds were recorded on a Jasco FTIR-300 E Fourier Transform Infrared Spectrometer.

The thermogravimetric analysis (TGA) of the polymeric materials were carried out through the use of the Thermogravimetric Analyzer (TGA) & Differential Scanning Calorimeter (DSC) – TA Instruments DSC SDT Q600. A sample weight of approximately 3 mg was employed at three heating rates (10, 15, and 20  $\text{K min}^{-1}$ ) under dry nitrogen gas. The advanced thermokinetics software package

AKTS-Thermokinetics, Ver. 4.15, was utilized for all kinetics analyses in this study.

### 2.3 Synthesis

#### 2.3.1 Synthesis Phenol-Terminated G0 Dendrimer 5

Dendrimer **5** has been synthesized in a two-step methodology [5]. The first step incorporates the Steglich esterification of the bimetallic complex **1** with a pentaerythritol core in order to isolate the G0 dendrimer **3** [5]. A 50 mL round-bottom flask was charged with pentaerythritol **2** (0.170 g, 1.27 mmol), **1** (5.28 g, 5.08 mmol), DMAP (0.500 g, 4.08 mmol), 10 mL of 3:1 DCM:DMSO solution. The solution was stirred and cooled in an ice bath to 0 °C within a nitrogen atmosphere while DCC (1.15 g, 5.59 mmol) was added over a 5-min period. The ice-bath was extracted after 5 min and the reaction mixture stirred in the same environment for 3 h at room temperature. Precipitated dicyclohexylurea (DCU) was removed by filtration through a Büchner funnel, and the filtrate was hydrolyzed in 50 mL of ice water to which  $\text{NH}_4\text{PF}_6$  (1.66 g, 10.2 mmol) was added. The product was removed with three 50-mL portions of a 5:1 DCM/DMF mixture. The extracts were washed with two 50-mL portions of 5% HCl and subsequently with two 50-mL portions of sodium bicarbonate, dried over  $\text{MgSO}_4$ , filtered, and the solvent removed with a rotary evaporator. The crude product of **3** was dissolved in acetone, cooled to – 25 °C in a freezer for 1 h, filtered to remove more DCU, and precipitated from the diethyl ether. The resulting yellow-green solid, **3**, was collected by suction filtration and dried under vacuum at room temperature.

The synthesis of dendrimer **5** followed a well-established chemistry [4]. A 50-mL round-bottom flask was charged with phenol (**4**) (0.76 g, 8.04 mmol), **3** (4.22 g, 1.00 mmol),  $\text{K}_2\text{CO}_3$  (4.87 g, 35.3 mmol), and 10 mL of DMF. The reaction mixture was stirred at room temperature for 16 h after flushing with nitrogen for an hour. Successively, the reaction mixture was poured into 300 mL of 10% HCl solution, and  $\text{NH}_4\text{PF}_6$  (1.66 g, 10.2 mmol) was added to precipitate the product. The product was filtered and dried under vacuum. Yield: (4.14 g, 93%).

#### 2.3.2 Synthesis of Crosslinked G0 Dendrimers 7 and 8

In a process parallel to the synthesis of **5**, dendrimers **7** and **8** were synthesized via the reaction of the G0 dendrimer **3** (4.22 g, 1.00 mmol) and hydroquinone **6** with a molar ratio of 1:4 to isolate dendrimer **7** and a ratio of 1:8 to produce dendrimer **8** [5]. The reactions were performed at room temperature for 16 h after flushing with nitrogen for an hour in the presence of  $\text{K}_2\text{CO}_3$  (4.87 g, 35.3 mmol) and 10 mL of DMF. The reaction mixture was subsequently poured

into 300 mL of 10% HCl solution, and  $\text{NH}_4\text{PF}_6$  (1.66 g, 10.2 mmol) was added to precipitate the product. The product was filtered and dried under vacuum. The chemical structure of dendrimer 5, dendrimer 7 and dendrimer 8 synthesized are shown in Fig. 1.

## 2.4 Thermal Analysis

The thermogravimetric analysis of the polymeric materials were carried out through the use of the Thermogravimetric

Analyzer (TGA) & Differential Scanning Calorimeter (DSC) – TA Instruments DSC SDT Q600. A sample weight of approximately 3 mg was employed at three heating rates (10, 15, and 20  $\text{K min}^{-1}$ ) under dry nitrogen gas. The advanced thermokinetics software package AKTS-Thermokinetics, Ver. 4.15, was utilized for all kinetics analyses in this study.

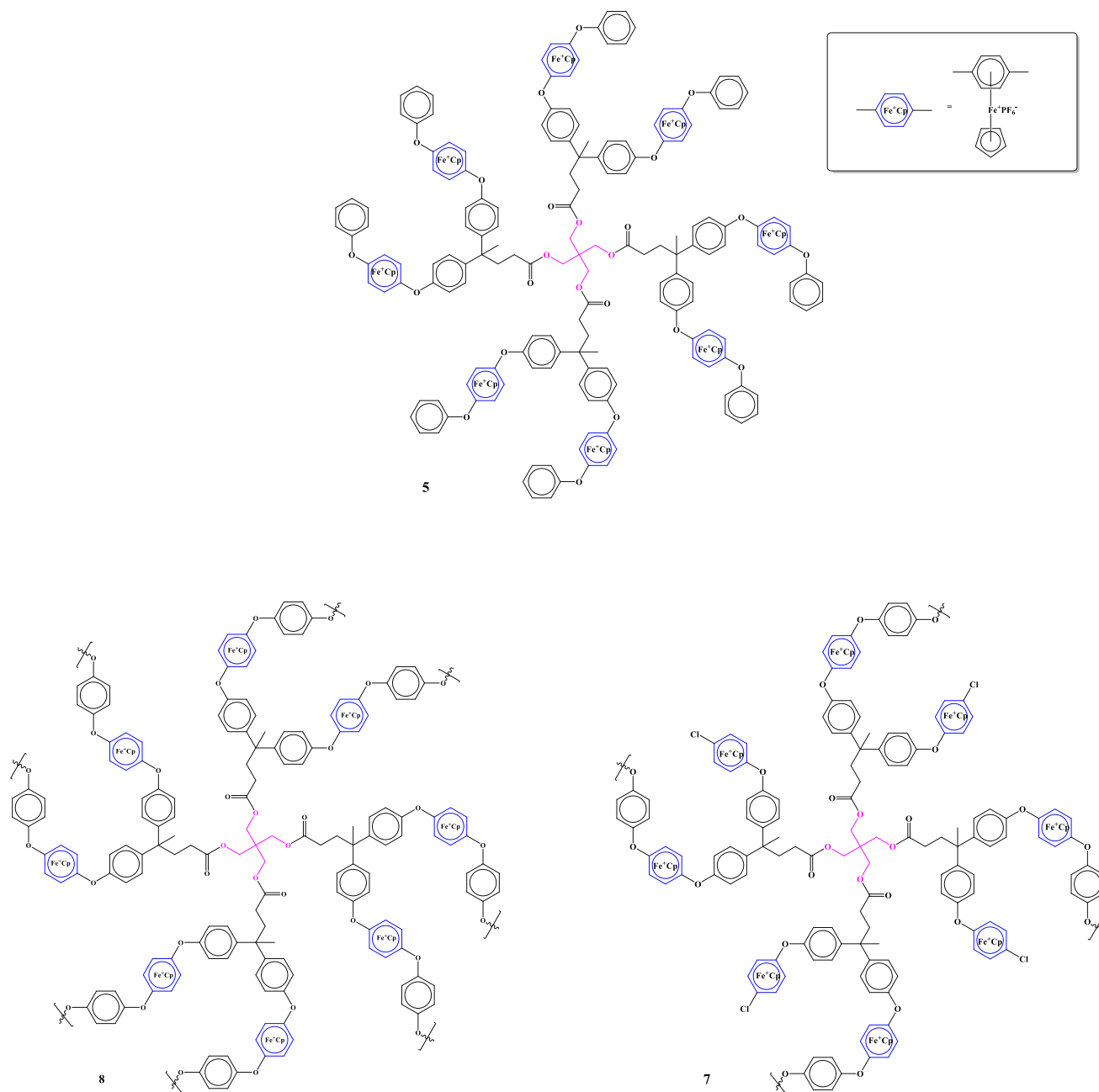


**Fig. 1** The chemical structure of dendrimer 5, dendrimer 7 and dendrimer 8

## 2.5 Kinetic Study

In the isoconversional method, the theoretical kinetic equation is combined with the Arrhenius expression, which interprets the DSC thermographs as a function of temperature ( $T$ ) expressed in terms of the conversion fraction (the reaction progress)  $\alpha$  as follows [5, 11, 12]:

$$\frac{d\alpha}{dt} = k(T)f(\alpha) = A(\alpha)f(\alpha) \exp\left(\frac{-E}{RT}\right), \quad (1)$$

where  $k$  is the reaction rate constant,  $A$  ( $s^{-1}$ ) is the pre-exponential (frequency) factor,  $E$  ( $\text{kJ mol}^{-1}$ ) is the apparent (effective) activation energy describing the overall of the phase change process,  $R$  is the universal gas constant and  $f(\alpha)$  is the reaction model (which describes the differential mechanisms of various kinetic model functions). In the thermogravimetric analysis (TGA),  $\alpha$  represents the weight loss fraction, which can be determined from the TG analysis as a fractional mass loss:

$$\alpha = \frac{m_0 - m_t}{m_0 - m_f}, \quad (2)$$

where  $m_0$ ,  $m_t$  and  $m_f$  represent the compound mass at the onset of degradation, at any time  $t$  and at the completion of degradation, respectively. For the nonisothermal conditions and when  $T$  is dependent on the heating rate ( $\beta$ ) and changes linearly with time ( $T = T_0 + \beta t$ ):

$$\beta = \frac{dT}{dt} = \text{constant}, \quad (3)$$

Hence, the isothermal condition Eq. (1) can be altered in terms of temperature dependency:

$$\frac{d\alpha}{dT} = \frac{A(\alpha)}{\beta} \exp\left(-\frac{E}{RT}\right) f(\alpha), \quad (4)$$

Integrating the aforementioned equation yields:

$$g(\alpha) = \int_0^\alpha \frac{d\alpha}{f(\alpha)} = \frac{A(\alpha)}{\beta} \int_{T_0}^T \exp\left(-\frac{E}{RT}\right) dT, \quad (5)$$

where  $g(\alpha)$  is the integral form of the reaction model, which does not possess an analytical solution in nonisothermal experiments. Thus, to solve this equation, a number of theoretical methodologies were obtained. The Flynn, Wall and Ozawa (FWO) method is one of these methods, which is measured at different but constant heating rates  $\beta_i$  [5, 11, 13, 14].

$$\ln(\beta_i) = \ln\left(\frac{AE_\alpha}{R}\right) - \ln(g(\alpha)) - 5.3305 - 1.0518 \frac{E_\alpha}{RT_{\alpha,i}}, \quad (6)$$

The plotting of  $\ln(\beta_i)$  against  $1/T_{\alpha,i}$  yields a straight line with a slope of  $-E_\alpha/R$ . The activation energy ( $E_\alpha$ ) and the pre-exponential ( $A_\alpha$ ) are subsequently determined from the slope and the intercept of the line, respectively.

## 2.6 Thermodynamic Study

The thermodynamic parameters demonstrate an integral role in furthering the understanding of the degradation of the organometallic dendrimers and their response to temperature and thermal stability. The thermodynamic parameters ( $\Delta H$ ,  $\Delta G$ , and  $\Delta S$ ) were calculated, utilizing the following equations [15–21]:

$$\Delta H = E_\alpha - RT_\alpha, \quad (7)$$

$$\Delta G = E_\alpha + RT \ln\left(\frac{K_B T}{hA}\right), \quad (8)$$

$$\Delta S = \frac{\Delta H - \Delta G}{T}, \quad (9)$$

where  $T$  is the absolute peak temperature,  $T_\alpha$  is the temperature at the degree of conversion  $\alpha$ ,  $h$  is the Planck constant ( $6.62 \times 10^{-34}$  Js) and  $K_B$  is the Boltzmann constant ( $1.381 \times 10^{-23}$  J K $^{-1}$ ).

## 3 Results and Discussion

### 3.1 The Degradation Behavior

The mass loss (TG) and derivative mass loss (DTG) curves were obtained under three different heating rates of 10, 15 and 20 °C min $^{-1}$ . The samples were heated from room temperature to 973 K. Our previous study [5] revealed that the three cross-linked organoiron dendrimers degradation exhibited different pyrolysis curves, but the overall changes were similar, according to TG curves. The dendrimers degradations was partitioned into two different steps. The low temperature degradation regime occurred at a temperature range of 403–504 K, accompanied by a loss of approximately 15%, whereas the high temperature degradation regime occurred at a temperature range of 542–862 K, accompanied by a loss of approximately 60%. Therefore, each degradation peak was treated as an individual peak. The first and second peaks are denoted as LTD and HTD, respectively. Figure 2 illustrates the TG and DTG curves of the three dendrimers under investigation.

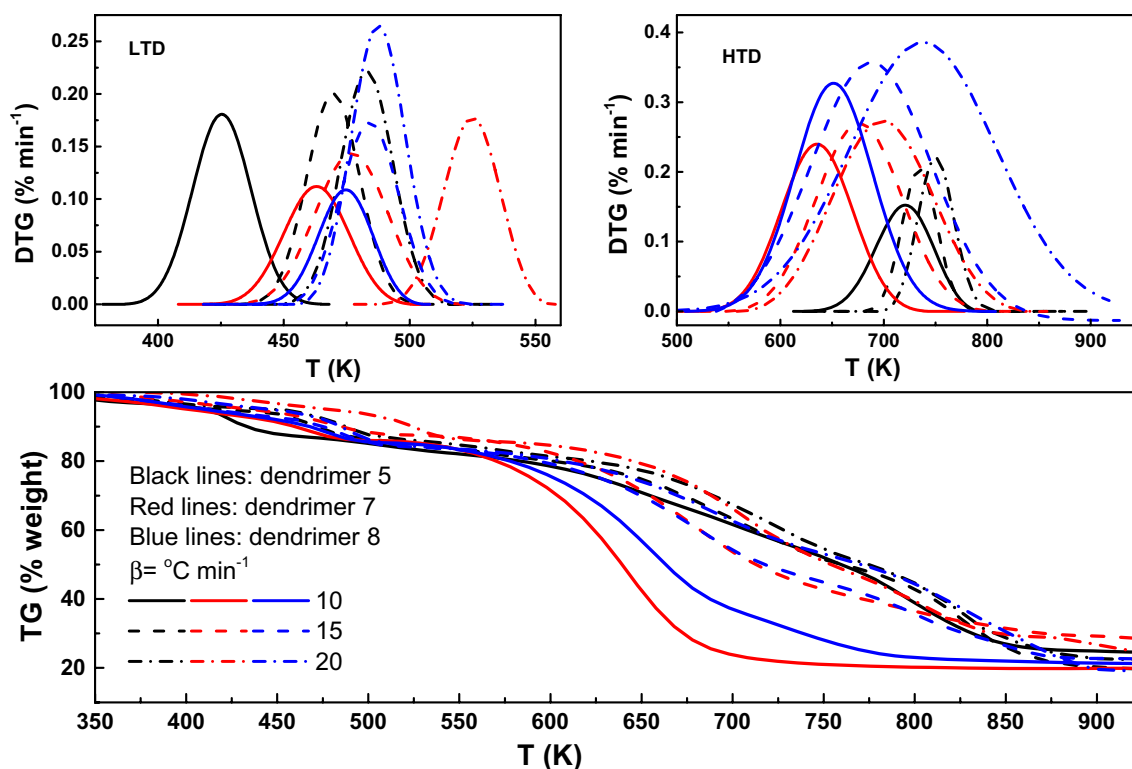


Fig. 2 The TG and DTG curves of dendrimer 5, dendrimer 7 and dendrimer 8 at heating rates 10, 15 and 20 °C min<sup>-1</sup>

### 3.2 Thermodynamic Parameters

The FWO Eq. (6) discussed above was employed to investigate the variation of the effective activation energy ( $E_{\alpha}(\alpha)$ ) with the conversion fraction ( $\alpha$ ) and temperature ( $E_{\alpha}(T)$ ), executed at different heating rates  $\beta_i$ . Figures 3, 4 and 5 present the calculated activation energies for the LTD and HTD steps. Correspondingly, these figures exhibit the variation of the logarithmic values of the pre-exponential factor ( $\ln(A_{\alpha})$ ). Furthermore, these values are in line with the values of the activation energy ( $E_{\alpha}(\alpha)$ ). These figures also disclosed a clear difference in the values of  $E_{\alpha}(\alpha)$  and  $E_{\alpha}(T)$  between the LTD and HTD steps. For the LTD step of dendrimer 5, there is a miniature increase (16–20 kJ mol<sup>-1</sup>) in the activation energy between the initial and final stage of the degradation while its increase in the HTD step is extremely high (50–140 kJ mol<sup>-1</sup>). Although the variation of  $E_{\alpha}(\alpha)$  for the LTD step of dendrimer 7 is equivalent to the LTD step of dendrimer 5, the HTD step of dendrimer 7 displays a slight decrease (43–34 kJ mol<sup>-1</sup>) with increasing  $\alpha$  or temperature. On the other hand, for dendrimer 8, the value of  $E_{\alpha}(\alpha)$  for the HTD step is almost constant with the  $\alpha$  or temperature, which is approximately 146 kJ mol<sup>-1</sup> exceptional at the terminal and final point. The value of the LTD step is less than the HTD step and decreases gradually with  $\alpha$

(51–26 kJ mol<sup>-1</sup>). Using the effective activation energies ( $E_{\alpha}$ ) and the pre-exponential factor ( $A_{\alpha}$ ), derived from the FWO model Eq. (6), the thermodynamic parameters ( $\Delta H$ ,  $\Delta G$ , and  $\Delta S$ ) were calculated, according to Eqs. 7, 8 and 9 mentioned above.

#### 3.2.1 The Change in Enthalpy

The change in enthalpy ( $\Delta H$ ) indicates the total heat transfer, i.e. characterizes the total amount of heat taken to decompose the dendrimer to the LTD step followed by decomposition to the HTD step. Figures 6 and 7 depict the variation of the changes in  $\Delta H$  as a function of the reaction progress ( $\alpha$ ) and temperature, respectively. As evident from these two figures,  $\Delta H$  of dendrimers 5 and 7 is approximately the same for the LTD step. Moreover, the variation of  $\Delta H$  with  $\alpha$  or  $T$  increases slightly as the reaction progress continues on.  $\Delta H$  exhibits a value of approximately 12 kJ mol<sup>-1</sup> at the beginning of the reaction and approximately 17 and 19 kJ mol<sup>-1</sup> for dendrimers 5 and 7 at the reaction end, respectively. This behavior is indicative of extremely low energy required to decompose dendrimers 5 and 7 for the LTD step. For dendrimer 8, the value of  $\Delta H$  for the LTD step is extremely high in evaluation with dendrimers 5 and 7 and almost constant at  $\alpha=0.5$  with a value of approximately 87 kJ mol<sup>-1</sup>. The LTD step is attributed to the loss of the cyclopentadienyl iron(II)

**Fig. 3** The values of  $E_{\alpha}(\alpha)$ ,  $\ln(A_{\alpha})$  and  $E_{\alpha}(T)$  of the LTD and HTD steps for dendrimer **5**

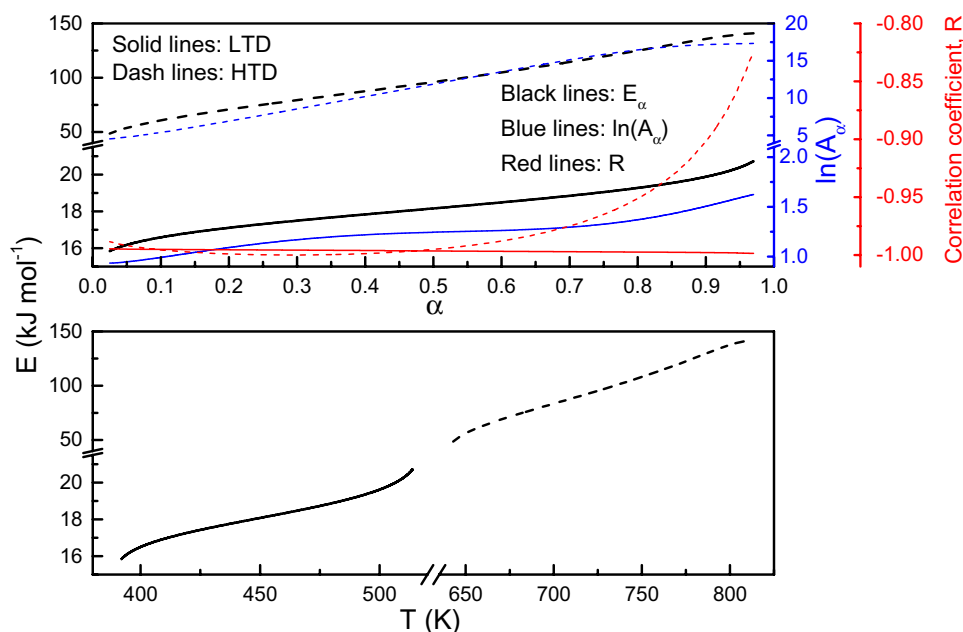
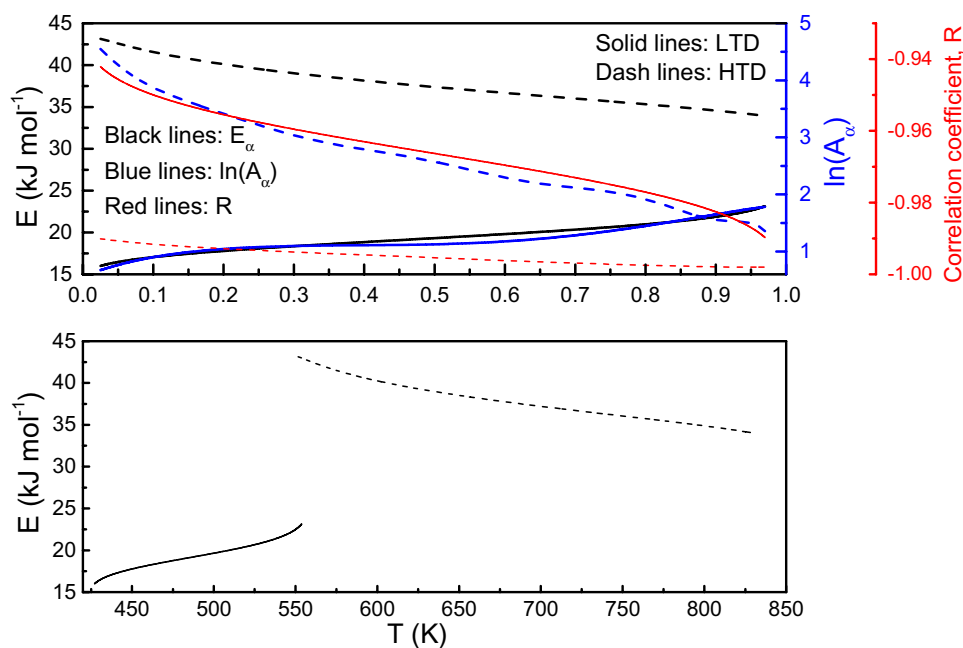


**Fig. 4** The values of  $E_{\alpha}(\alpha)$ ,  $\ln(A_{\alpha})$  and  $E_{\alpha}(T)$  of the LTD and HTD steps for dendrimer **7**

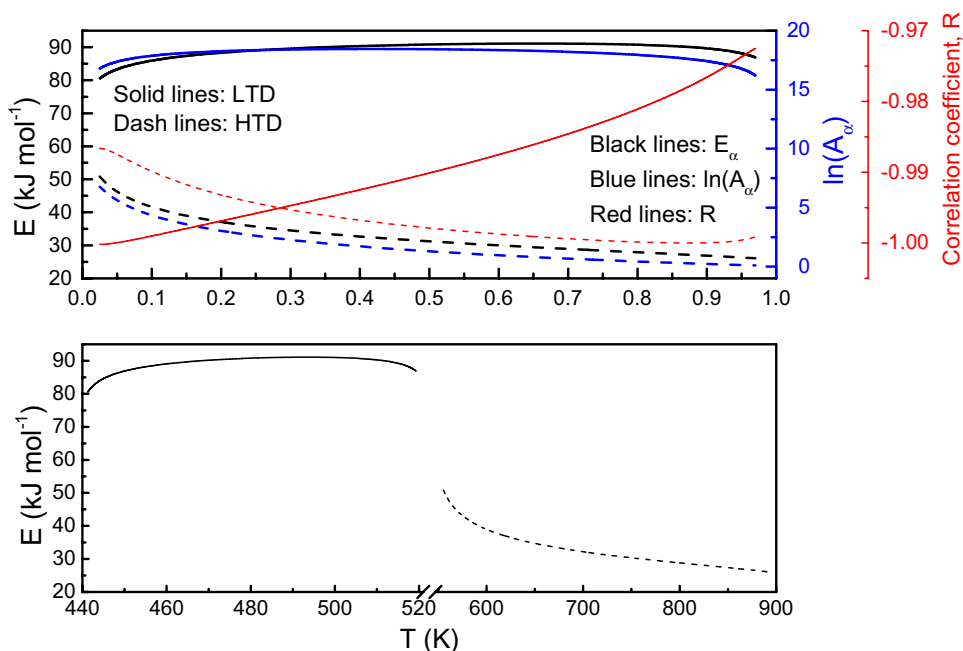


moiety attached to the terminals of the structure [5, 21]. The delay of degradation for dendrimers **7** and **8**, which occurred at a higher temperature in comparison to dendrimer **5** and is represented in Fig. 7 for the LTD step, was described in the basis of a number of cationic iron centers [5]. In addition, the high increase in the value of  $\Delta H$  for dendrimer **8** was assigned to the size and number of the peripheral groups.

However, the thermal decomposition of step 2 (HTD) for all three dendrimers proceeded through a different approach. As apparent from Figs. 6 and 7,  $\Delta H$  increased strongly alongside the increasing  $\alpha$  or  $T$  for dendrimer **5**.

At the initial stage of the reaction, the value of  $\Delta H$  for the HTD step was about  $39 \text{ kJ mol}^{-1}$ , which rises to approximately  $134 \text{ kJ mol}^{-1}$  at the terminal stage. This performance denotes the requirement of an elevated level of energy as the reaction grows. In contrast, for dendrimers **7** and **8**,  $\Delta H$  was found to possess a moderate value and gradually decreased with the increasing  $\alpha$  or  $T$ . The values of  $\Delta H$  for HTD are approximately 39 and  $52 \text{ kJ mol}^{-1}$  during the initial stage for dendrimers **7** and **8**, respectively. As the reaction progressed, these two values declined to approximately 27 and  $19 \text{ kJ mol}^{-1}$  at the terminal stage for dendrimers **7** and **8**,

**Fig. 5** The values of  $E_{\alpha}(\alpha)$ ,  $\ln(A_{\alpha})$  and  $E_{\alpha}(T)$  of the LTD and HTD steps for dendrimer **8**

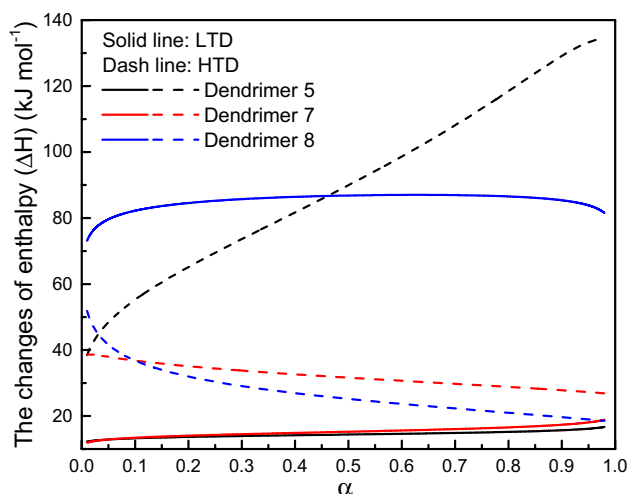


respectively. The perceptible shift to a high temperature and the increase to an elevated value of  $\Delta H$  for dendrimer **5** is ascribed to the breakage of the dendritic backbone and the presence of the phenolic peripheral groups, which is indicative of a higher thermal stability of such structure in appraisal with that of dendrimers **7** and **8**. The noticeable decrease in  $\Delta H$  for dendrimer **7** is ascribed to the existence of the activated chloride terminal, which is considered a good leaving group. Additionally, the bifunctionality of the hydroquinone, which has a high possibility of crosslinking, suggested the decrease in  $\Delta H$  for dendrimers **7** and **8**. From Fig. 6, it is palpable that the numbers of hydroquinone present affect the values of  $\Delta H$ , which are 31.81 and

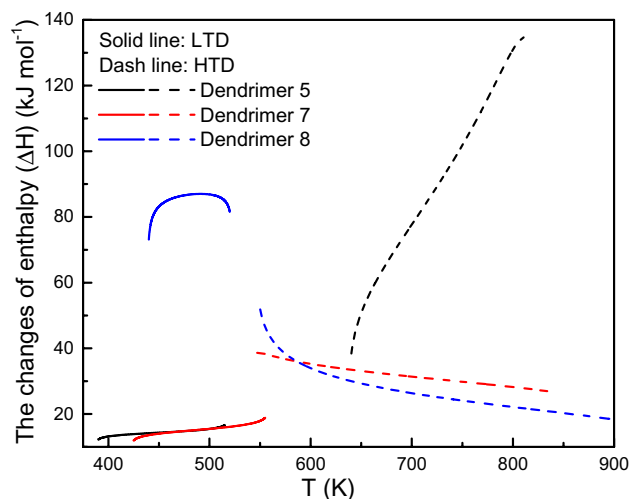
25.12  $\text{kJ mol}^{-1}$  at  $\alpha = 0.5$  for dendrimers **7** and **8** (where the number of hydroquinone groups are 4 and 8 for the two compounds), respectively.

### 3.2.2 The Change in the Gibbs Free Energy

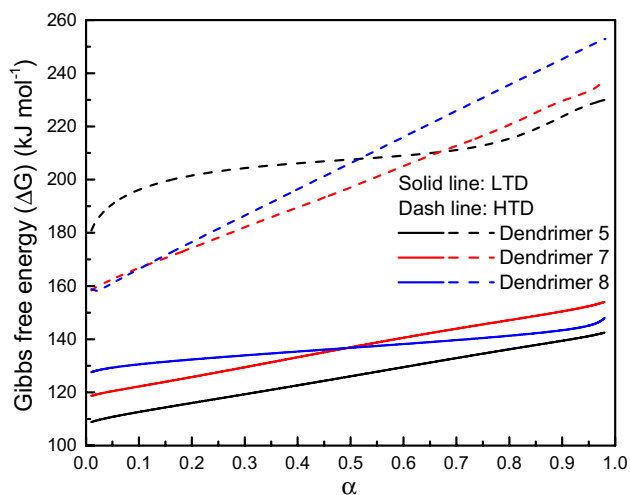
The difference between the free energy of a molecule and the free energies of its elements affords the change of the Gibbs free energy ( $\Delta G$ ) [18, 19]. For the LTD and HTD steps, Figs. 8 and 9 demonstrate the variation of  $\Delta G$  with the reaction conversion ( $\alpha$ ) and temperature, respectively. It is evident from these two figures that the  $\Delta G$  is higher for the HTD step in comparison with the LTD step and



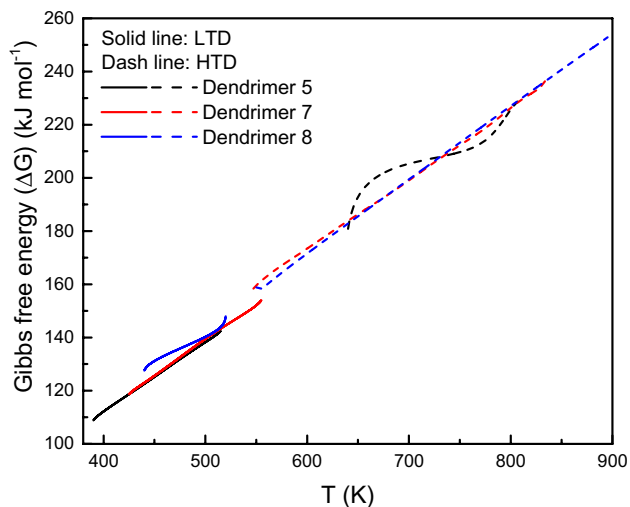
**Fig. 6** The variation of change in enthalpy ( $\Delta H$ ) as a function of the reaction progress ( $\alpha$ ) for the LTD and HTD steps for dendrimers **5**, **7** and **8**



**Fig. 7** The variation of change in enthalpy ( $\Delta H$ ) as a function of temperature for the LTD and HTD steps for dendrimers **5**, **7** and **8**

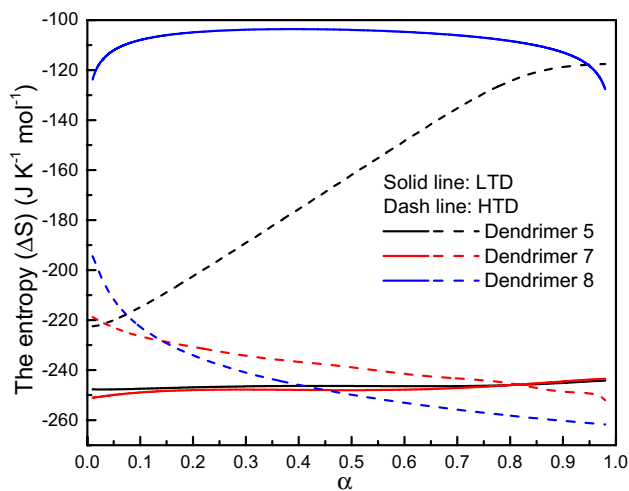


**Fig. 8** The variation of change in Gibbs free energy ( $\Delta G$ ) as a function of reaction progress ( $\alpha$ ) for the LTD and HTD steps for dendrimers 5, 7 and 8

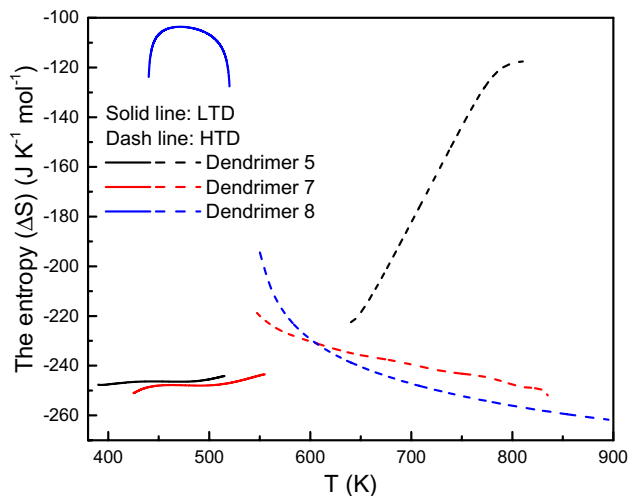


**Fig. 9** The variation of change in Gibbs free energy ( $\Delta G$ ) as a function of temperature for the LTD and HTD steps for dendrimers 5, 7 and 8

nearly in the same range for each step for the three dendrimers. Between the initial and final stages of the reaction and for the LTD step,  $\Delta G$  shifted within the ranges of 109–143, 119–154, and 128–148  $\text{kJ mol}^{-1}$  for dendrimers 5, 7, and 8, respectively. Alternatively, for the HTD step,  $\Delta G$  alternated within the ranges of 181–230, 159–236, and 159–253  $\text{kJ mol}^{-1}$  for the same dendrimers, respectively. Hence,  $\Delta G$  was discovered to be positive during the whole process, implying that the reaction is non-spontaneous and mandates external heat supply.



**Fig. 10** The variation of the entropy ( $\Delta S$ ) as a function of reaction progress ( $\alpha$ ) for the LTD and HTD steps for dendrimers 5, 7 and 8

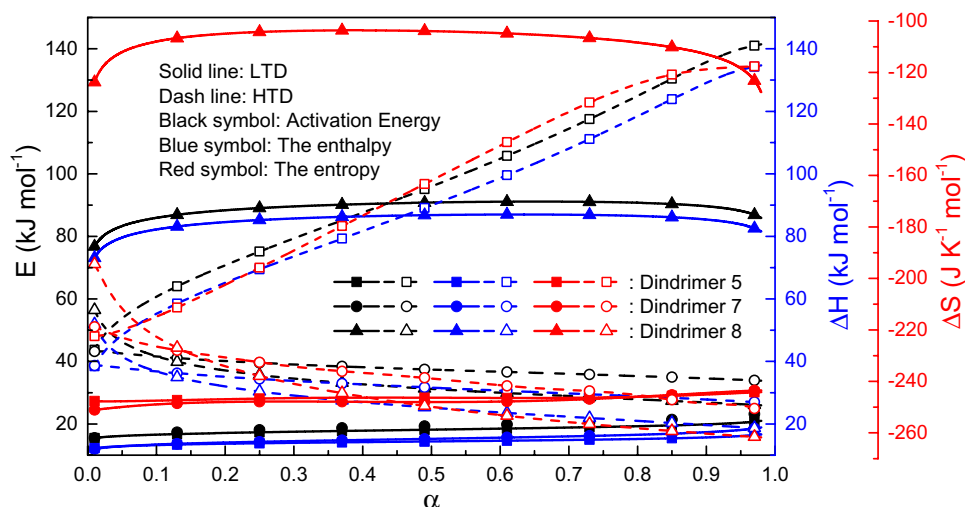


**Fig. 11** The variation of the entropy ( $\Delta S$ ) as a function of temperature for the LTD and HTD steps for dendrimers 5, 7 and 8

### 3.2.3 The Change in Entropy

Entropy ( $\Delta S$ ) is a physical property that is most commonly associated with the state function of the reaction system, reflecting the disorder, randomness or uncertainty of the system [16, 19]. Figures 10 and 11 establish the variation of  $\Delta S$  with the reaction conversion ( $\alpha$ ) and with temperature, respectively. It is apparent from these figures alongside Figs. 6 and 7 that the activation energy, enthalpy, and entropy exhibit the same tendency, which is represented in Fig. 12. Figure 10 illustrates that the values of  $\Delta S$  for the LTD and HTD steps proceed through a different methodology. On the other hand, the figure indicates that the values of  $\Delta S$  are negative for all samples under investigation for



**Fig. 12** The activation energy, enthalpy and entropy possessing the same tendency**Table 1** Kinetic and thermodynamic parameters for dendrimers 5

$\alpha$	$E_{\alpha}$ kJ mol <sup>-1</sup>	LTD					$E_{\alpha}$ kJ mol <sup>-1</sup>	HTD				
		A s <sup>-1</sup>	R <sup>2</sup>	$\Delta H$ kJ mol <sup>-1</sup>	$\Delta G$ kJ mol <sup>-1</sup>	$\Delta S$ J K <sup>-1</sup> mol <sup>-1</sup>		A s <sup>-1</sup>	R <sup>2</sup>	$\Delta H$ kJ mol <sup>-1</sup>	$\Delta G$ kJ mol <sup>-1</sup>	$\Delta S$ J K <sup>-1</sup> mol <sup>-1</sup>
0.1	16.6	2.70	0.9903	13.26	112.66	-247.45	60.72	$2.22 \times 10^2$	0.9911	55.26	196.22	-214.83
0.2	17.11	2.98	0.9910	13.67	116.02	-246.89	70.77	$1.01 \times 10^3$	0.9982	65.17	201.54	-202.45
0.3	17.5	3.22	0.9916	13.95	119.31	-246.49	79.35	$5.16 \times 10^3$	0.9999	73.61	204.33	-189.14
0.4	17.84	3.39	0.9922	14.18	122.65	-246.33	87.59	$2.70 \times 10^4$	0.9976	81.70	206.14	-175.58
0.5	18.16	3.47	0.9929	14.40	126.05	-246.35	95.98	$1.43 \times 10^5$	0.9902	89.65	207.57	-161.96
0.6	18.49	3.54	0.9936	14.62	129.49	-246.44	104.84	$7.46 \times 10^5$	0.9759	98.65	209.09	-148.40
0.7	18.85	3.65	0.9942	14.87	132.90	-246.40	114.44	$3.69 \times 10^6$	0.9506	108.11	211.14	-135.31
0.8	19.28	3.94	0.9949	15.19	136.20	-245.99	124.94	$1.40 \times 10^7$	0.9048	118.46	215.37	-124.40
0.9	19.89	4.51	0.9958	15.69	139.42	-245.09	135.72	$2.82 \times 10^7$	0.8134	129.10	223.91	-118.77

**Table 2** Kinetic and thermodynamic parameters for dendrimers 7

$\alpha$	$E_{\alpha}$ kJ mol <sup>-1</sup>	LTD					$E_{\alpha}$ kJ mol <sup>-1</sup>	HTD				
		A s <sup>-1</sup>	R <sup>2</sup>	$\Delta H$ kJ mol <sup>-1</sup>	$\Delta G$ kJ mol <sup>-1</sup>	$\Delta S$ J K <sup>-1</sup> mol <sup>-1</sup>		A s <sup>-1</sup>	R <sup>2</sup>	$\Delta H$ kJ mol <sup>-1</sup>	$\Delta G$ kJ mol <sup>-1</sup>	$\Delta S$ J K <sup>-1</sup> mol <sup>-1</sup>
0.1	17.05	2.46	0.9025	13.42	122.24	-248.92	41.57	48.14	0.9833	36.80	166.77	-226.46
0.2	17.80	2.84	0.9129	14.05	125.77	-247.98	40.11	30.43	0.9858	35.09	174.32	-230.69
0.3	18.36	2.99	0.9207	14.50	129.46	-247.79	39.03	20.87	0.9876	33.77	182.08	-234.23
0.4	18.85	3.03	0.9274	14.88	133.22	-247.91	38.16	16.28	0.9892	32.64	189.54	-236.67
0.5	19.32	3.08	0.9337	15.24	136.95	-248.01	37.39	13.08	0.9908	31.63	197.06	-238.86
0.6	19.81	3.24	0.9401	15.62	140.55	-247.81	36.69	9.95	0.9924	30.68	205.10	-241.48
0.7	20.34	3.61	0.9468	16.04	143.94	-247.14	36.01	8.32	0.9937	29.76	212.72	-243.30
0.8	20.97	4.25	0.9547	16.56	147.17	-245.98	35.33	6.78	0.9950	28.83	220.59	-245.32
0.9	21.88	5.21	0.9654	17.36	150.46	-244.51	34.57	4.74	0.9958	27.83	259.56	-248.62

**Table 3** Kinetic and thermodynamic parameters for dendrimers 8

$\alpha$	$E_a$ kJ mol <sup>-1</sup>	LTD					$E_a$ kJ mol <sup>-1</sup>	HTD				
		A s <sup>-1</sup>	R <sup>2</sup>	$\Delta H$ kJ mol <sup>-1</sup>	$\Delta G$ kJ mol <sup>-1</sup>	$\Delta S$ J K <sup>-1</sup> mol <sup>-1</sup>		A s <sup>-1</sup>	R <sup>2</sup>	$\Delta H$ kJ mol <sup>-1</sup>	$\Delta G$ kJ mol <sup>-1</sup>	$\Delta S$ J K <sup>-1</sup> mol <sup>-1</sup>
0.1	85.96	$5.81 \times 10^7$	0.9980	82.23	130.55	-107.96	41.62	76.92	0.9799	36.78	166.43	-222.68
0.2	88.35	$8.54 \times 10^7$	0.9938	84.56	132.37	-104.92	37.11	20.72	0.9865	31.97	176.57	-234.08
0.3	89.59	$9.88 \times 10^7$	0.9895	85.73	133.92	-103.86	34.51	9.59	0.9906	29.07	186.50	-240.95
0.4	90.35	$1.03 \times 10^8$	0.9850	86.42	135.36	-103.62	32.67	5.57	0.9936	26.94	196.37	-245.92
0.5	90.82	$1.01 \times 10^8$	0.9803	86.83	136.76	-103.93	31.22	3.66	0.9958	25.20	206.21	-249.83
0.6	91.07	$9.39 \times 10^7$	0.9752	87.01	138.18	-104.71	30	2.60	0.9975	23.68	216.04	-253.05
0.7	91.08	$8.11 \times 10^7$	0.9694	86.95	139.66	-106.07	28.92	1.96	0.9988	22.30	225.86	-255.80
0.8	90.75	$6.25 \times 10^7$	0.9625	86.55	141.30	-108.37	27.90	1.54	0.9997	20.98	235.63	-258.18
0.9	89.66	$3.67 \times 10^7$	0.9537	85.39	143.37	-112.93	26.87	1.25	0.9999	19.66	245.30	-260.25

both the LTD and HTD steps, signifying that the system is becoming less disordered and that this degradation does not occur spontaneously. The negative values of  $\Delta S$  are observed in many studies [5, 15–19]. Tables 1, 2, and 3 present a summary of the thermodynamic parameters for the LTD and HTD steps for all three dendrimers under investigation.

## 4 Conclusions

The experimental results of the TGA curves demonstrated two phases of mass loss for all three analyzed dendrimers with about 15% and 60% loss for the first and second degradations. The effective activation energies and the pre-exponential factors, derived from the Flynn, Wall and Ozawa (FWO) model, were employed to quantify the thermodynamic parameters (the changes in enthalpy ( $\Delta H$ ), Gibbs free energy ( $\Delta G$ ) and entropy ( $\Delta S$ )). For the LTD step of all three dendrimers, the thermodynamic parameters of enthalpy and the entropy approximately exhibited a constant trend with a higher conversion fraction ( $\alpha$ ) and/or temperature, which proposed that the degradations were constant in progress during the reaction. For the HTD step, these two parameters revealed a distinct and noticeable increasing trend with the upsurge of  $\alpha$  and/or temperature for dendrimer 5, intimating that the degradation proceeded with difficulty during the reaction. On the contrary, for dendrimers 7 and 8, the changes in enthalpy and entropy for the HTD steps disclosed a slightly decreasing trend with a higher conversion fraction ( $\alpha$ ) and/or temperature, which suggested that the degradation of both dendrimers proceeded with ease during the reaction. Lastly, for all three dendrimers, the change in the Gibbs free energies ( $\Delta G$ ) for the two steps were discovered to be positive

during the whole process, indicating that the degradations are non-spontaneous and necessitate external heat supply.

**Funding** The authors have not disclosed any funding.

## Declarations

**Competing Interests** The authors have not disclosed any competing interests.

## References

- M.J. Dunlop, C. Agatemor, A.S. Abd-El-Aziz, R. Bissessur, Nanocomposites derived from molybdenum disulfide and an organoiron dendrimer. *J. Inorg. Organomet. Polym. Mater.* **27**(Suppl. 1), S84–S89 (2017)
- A.S. Abd-El-Aziz, C. Agatemor, Emerging opportunities in the biomedical applications of dendrimers. *J. Inorg. Organomet. Polym. Mater.* **28**, 369–382 (2018)
- M. Heidarizadeh, E. Doustkhah, F. Saberi, S. Rostamnia, A. Hassankhani, P.F. Rezaei, Y. Ide, Silica nanostructures, a heterogeneous surface for dendrimer functionalization. *ChemistrySelect* **3**, 7137–7151 (2018)
- M. Alsehli, S.Y. Al-Raqa, I. Kucukkaya, P.R. Shipley, B.D. Wagner, A.S. Abd-El-Aziz, Synthesis and photophysical properties of a series of novel porphyrin dendrimers containing organoiron complexes. *J. Inorg. Organomet. Polym. Mater.* **29**, 628–641 (2019)
- A.A. Joraid, R.M. Okasha, M.A. Al-Maghrabi, T.H. Afifi, C. Agatemor, A.S. Abd-El-Aziz, Thermal degradation behavior of a new family of organometallic dendrimer. *J. Inorg. Organomet. Polym. Mater.* **30**, 2937–2951 (2020)
- P.A. Chase, R.J.M. Klein Gebbink, G. van Koten, Where organometallics and dendrimers merge: the incorporation of organometallic species into dendritic molecules. *J. Organomet. Chem.* **689**, 4016–4054 (2004)
- B.V. Lebedev, M.V. Ryabkov, E.A. Tatarinova, E.A. Rebrov, A.M. Muzafarov, Thermodynamic properties of the first to

- fifth generations of carbosilane dendrimers with allyl terminal groups. *Russ. Chem. Bull.* **52**, 545–551 (2003)
8. N.N. Smirnova, O.V. Stepanova, T.A. Bykova, A.V. Markin, A.M. Muzafarov, E.A. Tatarinova, V.D. Myakushev, Thermodynamic properties of carbosilane dendrimers of the third to the sixth generations with terminal butyl groups in the range from T→0 to 600 K. *Thermochim. Acta* **440**, 188–194 (2006)
  9. M.A. Gonzalez-Fuentes, J. Manriquez, R. Antano-Lopez, L.A. Godinez, Kinetic and thermodynamic study of the transfer of anionic polyamidoamine dendrimers across two immiscible liquids. *Electrochim. Acta* **56**, 8299–8304 (2011)
  10. A.V. Markina, Y.A. Sarmini, S.S. Sologubov, N.N. Smirnova, K.L. Boldyrev, E.A. Tatarinova, I.B. Meshkov, A.M. Muzafarov, Thermodynamic properties of a first-generation siloxane dendrimer with terminal trimethylsilyl groups. *Russ. J. Phys. Chem. A* **94**, 240–248 (2020)
  11. S. Vyazovkin, A.K. Burnham, J.M. Criado, L.A. Perez-Maqueda, C. Popescu, N. Sbirrazzuoli, ICTAC Kinetics Committee recommendations for performing kinetic computations on thermal analysis data. *Thermochim. Acta* **520**, 1–19 (2011)
  12. A.A. Joraid, I.M.A. Alhosuini, Effect of heating rate on the kinetics and mechanism of crystallization in amorphous  $\text{Se}_{85}\text{Te}_{10}\text{Pb}_5$  glasses. *Thermochim. Acta* **595**, 28–34 (2014)
  13. T.A. Ozawa, A new method of analyzing thermogravimetric data. *Bull. Chem. Soc. Jpn.* **38**, 881–1886 (1965)
  14. J.H. Flynn, L.A. Wall, Thermal analysis of polymer by thermogravimetric analysis. *J. Res. Natl. Bur. Stand. Sect. A* **70**, 487–523 (1966)
  15. A.S. Khan, Z. Man, M.A. Bustam, C.F. Kait, Z. Ullah, A. Nasrullah, M.I. Khan, G. Gonfa, P. Ahmad, N. Muhammad, Kinetics and thermodynamic parameters of ionic liquid pretreated rubber wood biomass. *J. Mol. Liq.* **223**, 754–762 (2016)
  16. X. Yuan, T. He, H. Cao, Q. Yuan, Cattle manure pyrolysis process: kinetic and thermodynamic analysis with isoconversional methods. *Renew. Energy* **107**, 489–496 (2017)
  17. P. Sharma, P. Uniyal, Investigating thermal and kinetic parameters of lithium titanate formation by solid-state method. *J. Therm. Anal. Calorim.* **128**, 875–882 (2017)
  18. W. Zhang, Z. Li, L. Shi, Z. Li, Y. Luo, Q. Liu, R. Huang, Methyltrichlorosilane modified hydrophobic silica aerogels and their kinetic and thermodynamic behaviors. *J. Sol-Gel Sci. Technol.* **89**, 448–457 (2019)
  19. V. Vasudev, X. Ku, J. Lin, Pyrolysis of algal biomass: Determination of the kinetic triplet and thermodynamic analysis. *Biore-source Technol.* **317**, 124007 (2020)
  20. S. Singh, J.P. Chakraborty, M.K. Mondal, Intrinsic kinetics, thermodynamic parameters and reaction mechanism of non-isothermal degradation of torrefied *Acacia nilotica* using isoconversional methods. *Fuel* **259**, 116263 (2020)
  21. A.A. Joraid, S.Y. Al-Raqa, Kinetic and thermodynamic studies of phase transition from hexagonal to discotic liquid crystal in metal-free 1,4,8,11,15,18,22,25-octahexylphthalocyanine. *Liq. Cryst.* **48**, 1709–1722 (2021)

**Publisher's Note** Springer Nature remains neutral with regard to jurisdictional claims in published maps and institutional affiliations.